

CERN - European Laboratory for Particle Physics

CERN/PS/HI 88-72

DESIGN OF THE PREINJECTOR FOR THE CERN RFQ2 PROJECT

Ch. Hill, K. Prelec\* and M. Weiss

\*visitor at CERN in 1987, from BNL

## DESIGN OF THE PREINJECTOR FOR THE CERN RFQ2 PROJECT

Ch. Hill, K. Prelec,<sup>\*</sup> and M. Weiss

### Summary

A preinjector for the RFQ2 project containing a DP (duoplasmatron) ion source and a beam extraction and acceleration system has been studied. The system has to deliver more than 250 mA of protons with a normalized emittance of  $\sim 1.5 \pi$  mm mrad and of such a form to be easily accepted and handled by the subsequent low energy beam transport system.

Central to the study was the computer program BEAM obtained a few years ago from USA and, with some minor modifications, put into operation at CERN. In order to obtain results one can rely on, it was necessary to analyze and understand the way ion source plasma parameters are treated in the program. Realistic values of plasma parameters were selected using both, theoretical considerations and experimental results; effects of varying these parameters were then checked. Finally, the geometry of the extraction and acceleration system was optimized.

---

<sup>\*</sup> On leave from Brookhaven National Laboratory, Upton, NY USA.

## 1. Introduction

The study of a beam extraction and acceleration system, usually called dc column, is an important part in the design of low energy accelerators. The region close to the ion source is particularly delicate as the particles start there with very low velocities and are accelerated in strong electrostatic fields. In the boundary region (sheath) there must exist an equilibrium between the source plasma and the external electrostatic field. The motion of charged particles has to simultaneously satisfy the Poisson equation and the Vlasov equation. Solutions are found numerically by iteration processes and it is the availability of adequate computer programs which makes such an analysis possible.

More than 20 years ago one of the pioneering programs in this field was written at CERN<sup>1</sup> at the request of the Linac Group. Many features of this program have been appreciated and later used in other, more sophisticated programs rendered possible by the advent of computers with rapidly growing speeds of computation. The main effort in more recent programs has been put into finding consistent solutions for the motion of charged particles in electrostatic fields, including the transition region between the neutral plasma (equality of electron and ion densities,  $n_e = n_i$ ) and the ion beam ( $n_e = 0$ ).

At the time of construction of RFQ1, B. Hamm, then at LANL, was using the program SNOW,<sup>2</sup> which worked to a certain extent according to requirements outlined above. The dc column for the RFQ1 was designed with the program SNOW. Its performance was satisfactory and in reasonable agreement with expectations. Since then, the programming techniques have improved and through the courtesy of B. Hamm we have obtained the program BEAM,<sup>3</sup> which has been used for the RFQ2 project.

The requirements of the dc column of RFQ2 are as follows: acceleration to an energy of 90 keV (this is a compromise between space charge

problems and high voltage problems) of a proton beam of  $\geq 250$  mA. As in the beam coming out of our DP ion source only about 80% of ions are protons, the dc column must be capable of handling the correspondingly higher total currents. These requirements could be met after an extensive use of program BEAM; several shortcomings of the program have been overcome and a good knowledge of the importance and mutual dependence of various parameters has been gained.

## 2. Use of the Program BEAM

The descriptions of the program BEAM that were available<sup>4,5</sup> were not sufficient for a straightforward and reliable use. Only after a considerable number of runs and minor corrections to the program itself, did reliable results begin to show up. As already mentioned, the program starts by considering the plasma and its boundary and it is felt worthwhile to devote a separate section (2.1) to this subject. In the following section (2.2) we report the experience we gained from using BEAM. Only after this preliminary work could the design of the dc column be carried out.

The program BEAM, which is two-dimensional, has in our case been used for a cylindrical geometry with rotational symmetry (r-z plane). The relevant beam parameters, as e.g. the transverse second momenta, are computed in the r, r' phase plane (there are no azimuthal velocity components in the beam). To obtain the momenta in the cartesian coordinates we are used to working with, the r, r' results have simply to be divided by 2. The integration of equations of motion is done in the program by the Bulirsch-Stoer<sup>6</sup> method. This method uses a variable, adjustable integration step length. At the end, the integration is terminated before the step goes over the integration limit. As a consequence, the beam trajectories finish at distances somewhat shorter than the region under analysis. The program checks the convergence just before the end of the region, but as some of the rays have already been discontinued

there, a source of error is introduced in the calculation of beam characteristics. This error is avoided by choosing the beam check point sufficiently before the specified end of the region.

The beam characteristics are computed not only for the total beam, but also for a specified number of beam fractions. A beam fraction is obtained by leaving out a certain percentage of outermost particles in the beam emittance. In this way a good knowledge of the current density distribution is obtained.

## 2.1 Extraction of Positive Ions from the Plasma

The DP ion source with its expansion cup and the dc accelerating column is schematically shown in Fig. 1. The plasma in the expansion cup serves as a source of positive ions to be extracted and accelerated by the outside electrostatic field. The program BEAM calculates the potential distribution and a certain number of particle trajectories starting at the plasma-sheath boundary (emitting surface). The motion of ions is computed in the outside electrostatic field corrected for the presence of the ion space charge, as well as the electron space charge.

The initial parts of ion trajectories, from the plasma-sheath boundary (i.e. the plane where the neutrality requirement  $n_e = n_i$  is still satisfied) and through the sheath requires in principle a simultaneous solution of two partial differential equations, Poisson's equation for the electrostatic potential  $\phi$

$$\nabla^2 \phi = - \frac{\rho e}{\epsilon_0},$$

where  $\rho$  is the total (ion and electron) space charge density, and Vlasov's equation for the ion velocity distribution function  $f_1(\vec{v})$  or for the ion density distribution,  $n_1 = \int f_1(\vec{v}) d\vec{v}$ .<sup>7</sup> Poisson's equation can be written as

$$\nabla^2 \phi = \frac{-e}{\epsilon_0} \left\{ n_i - n_{e0} \exp \left( -e \frac{\phi_0 - \phi}{kT_e} \right) \right\} .$$

The electron space charge term on the right-hand side of the equation corresponds to a Maxwellian distribution of electron energies with a temperature  $T_e$  and density  $n_{e0}$  in the center of the plasma; the potential  $\phi$  is lower (decelerating for electrons) than the potential  $\phi_0$  in the unperturbed plasma. The sheath edge (adjacent to the plasma) is assumed to be the ion emitting surface, where the trajectory begins. At this position the plasma is still neutral

$$n_i = n_e = n_{e0} \exp \left( -e \frac{\phi_0 - \phi_s}{kT_e} \right) = n_{e0} \exp (-\eta_s),$$

where  $\eta_s = (\phi_0 - \phi_s)/kT_e$  is the normalized difference between the potential  $\phi_0$  in the center of the plasma and potential  $\phi_s$  at the sheath edge. Self<sup>8</sup> has analyzed the plasma-sheath problem; his value of  $\eta_s$  equal to 0.8539 corresponds to the extreme limit of applicability of the plasma approximation to the sheath. In the program BEAM a value of  $\eta_s = \ln 2$  has been used, corresponding to the Bohm<sup>9</sup> sheath criterion which, for a stable sheath region, imposes on ions reaching the sheath a minimum kinetic energy

$$m_i v_i^2 > k_e T_e .$$

It should be noted that the plasma density  $n_{e0}$  in the center of the discharge, far from the sheath, is higher than the density at the sheath edge  $n_i = n_e = n_{e0} \exp (-\eta_s)$ .

To begin the calculation of ion trajectories at the sheath edge, one has to know some plasma parameters and to make, in addition, some assumptions. The electron energy distribution is assumed to be Maxwellian, with a temperature  $T_e$ . To specify the ion emitting properties of the sheath edge, the program BEAM assumes that the ion energy distribution is

also Maxwellian with a temperature  $T_i$ . The ion density at the sheath edge is

$$n_i = n_{e0} \exp(-\eta_s) \quad ,$$

and the ions have there a drift velocity  $v_D$  perpendicular to the sheath edge. The approach selected in the program starts with a given ion current density  $j_+(\eta_s)$  distribution at the sheath edge which is a function of the distance from the beam axis. This distribution can be determined experimentally by electrostatic probe measurements on the source itself, in the ion saturation region.<sup>10</sup> From the probe characteristics one can also determine the electron temperature  $T_e$ .<sup>10</sup> Calculations by Self<sup>8</sup> show that the initial ion current density  $j_+(\eta_s)$  at the sheath edge is related to the center plasma density  $n_{e0}$  and to the electron temperature  $T_e$  by the expression:

$$j_+(\eta_s) = n_{e0} e I(\eta_s) \sqrt{\frac{2kT_e}{n_i}} \quad .$$

Values of the function  $I(\eta_s)$  have been computed by Self<sup>8</sup> (for  $\eta_s=0.8539$ ,  $I(\eta_s) = 0.3444$ ), but in the program we use  $I(\eta_s) = I(\ln 2) \cong \frac{1}{2\sqrt{\pi}} = 0.282$ . The current density at the sheath edge and the drift velocity  $v_D$  are connected through

$$j_+(\eta_s) = n_i(\eta_s) e v_D = n_{e0} \exp(-\eta_s) e v_D \quad ,$$

so that

$$v_D = \exp(\eta_s) I(\eta_s) \sqrt{\frac{2kT_e}{n_i}} \quad .$$

Therefore, the drift velocity  $v_D$  can be calculated if the electron temperature is known. The program also takes into account the possibility that all ions have an additional initial directed velocity, e.g. due to a step  $V_i$  in the potential before the expansion cup. This velocity component is then just added to the value  $v_D$  calculated above.

Once the value of  $v_D$  is known, it is possible to calculate the density  $n_{eo}$  in the center of the plasma:

$$n_{eo} = \frac{j_+ (\eta_s)_{r=0}}{e v_D} \exp (\eta_s) \quad .$$

This is then followed by the calculation of one of the fundamental plasma parameters, the Debye length  $\lambda_D$ :

$$\lambda_D = \sqrt{\frac{\epsilon_0 kT_e}{n_{eo} e^2}} \quad ,$$

which, in the program, serves to normalize space variables and to position the sheath edge with respect to the first electrode, see Fig. 1. The program deals with a discrete number of ion orbits distributed (in the case of a cylindrical geometry) in cells along the radius of the sheath edge, i.e. of the ion emitting surface. A current density is specified for each cell, the cells being of equal length radially. Within each cell a certain number of orbits,  $2 i_p$ , are selected. They originate from  $2 i_p$  equidistant points within the cell. In order to represent all ions crossing the sheath edge adequately, the ion velocity distribution function (which is assumed to be Maxwellian, possibly with an initial constant component added to all ions) is divided into  $i_p$  velocity space volumes, each containing or representing equal number of ions. The program integrates the distribution function within each of the  $i_p$  velocity space volumes searching for the lower and upper limits of integration such that the number of ions in any volume is always the same. Once the limits of integration for all the  $i_p$  volumes have been determined, initial radial and axial momentum components are computed by averaging the corresponding momenta (using the ion velocity distribution function) over individual velocity space volumes. Initial values of average momenta (radial and axial) are then assigned to initial positions of orbits in such a way that the point (within a cell) closest to the beam axis has the largest converging radial momentum and the point furthest away from the beam axis the largest diverging radial momentum.



To account for different values of emitted current density  $j_+(r)$  from cell to cell, each orbit will eventually be represented by a value proportional to the product of the current density within the cell and the mean radius of the cell.

The position of the emitting surface or the plasma sheath edge, is initially arbitrarily set at a distance upstream of the first electrode. In the initial phase of the program, the emitting surface is then moved with respect to the first electrode by an amount equal to a selected multiple,  $m_\ell$ , of the Debye length  $\lambda_D$  (calculated from  $j_+$  and  $v_D$ ). A judgment of the validity of the selected  $m_\ell$  can be made by analyzing the potential distribution or electrical field in the vicinity of the emitting surface as calculated by the program. The shape of the potential and field should correspond to a space charge limited flow, see Figure 2.

A correct position of the emitting surface will result in conditions closest to the real situation, but not necessarily in best calculated beam parameters.

## 2.2 Selection of Input Parameters

The input parameters of the program can be grouped into three categories: parameters related to the computation itself (mesh size, relaxation coefficients, required accuracy, etc.), plasma parameters, and ion optical system parameters (shape and distances of electrodes, electrode potentials, current density distribution on the plasma sheath, etc.).

### 2.2.1 Computation Parameters

Most of these parameters have been determined by trial and suggested values given in the instructions for the use of the program BEAM.<sup>5</sup> There is a certain freedom in selecting the numbers of mesh lines, within the limits described in Ref. 5. It is, however, important that the mesh size in the radial direction (perpendicular to the axis) coincides with the cell sizes for the current density distribution. In

the axial direction there is a possibility of having a variable mesh size. This is very important as one can have reduced steps in the vicinity of the ion emitter, where the ion velocities are the smallest and the space charge density the highest. The variable mesh size is specified by a factor  $m_s$  which is defined as

$$z' = \frac{1}{m_s} \ln (1 + m_s z) \quad ,$$

where  $z'$  is the new, transformed axial variable in which the mesh size is again equal. Note that in the program one works with distances normalized to  $\lambda_D$ , so any change in  $\lambda_D$  modifies the longitudinal mesh size. Running otherwise identical programs and varying only the parameter  $m_s$ , one finds that the output does not change if  $m_s > 0.002$ . We have, therefore, selected the value of  $m_s = 0.002$  for the final calculations. Figure 3 shows our reference electrode geometry in the transformed coordinate system, for different values of  $m_s$ ; Fig. 4 shows output beam emitances,  $E(I)$ , with  $m_s$  as parameters.

### 2.2.2 Plasma Parameters

Before optimizing the shape and position of electrodes we have tried to estimate the importance of plasma parameters on the calculation of beam parameters, i.e. on  $E(I)$ . Comparing curves of  $E(I)$  was a convenient way of judging the effects of the change of a particular parameter. The following computer studies were done for a reference system of electrodes shown in Fig. 3 and described in 2.2.3.

The plasma has a potential  $V_p$  and such potentials in the expansion cup, relative to the source anode, have been measured by G. Gautherin et al.<sup>11</sup> using an emitting probe. In the program BEAM, essentially two values of  $V_p$  have been tried out (5 and 15 V) with a negligible effect on beam parameters. This is understandable since  $V_p$  is used to define the potential of the ion emitter with respect to other

electrodes in the system, and a few tens of volts compared to kilovolts have only a very small effect on ion orbits.

Ion energy distributions are represented by two parameters, the ion temperature  $T_i$  and the energy component  $eV_i$  corresponding to the common directed velocity  $v_D$ . Energy spectra of ions leaving the expansion cup of a duoplasmatron source have been measured by several authors.<sup>11,12</sup> The shape of the spectra depends, among other things, on the configuration of the magnetic field in the cup and on the bias on the cup walls. There seems to be two groups of ions, one with energies indicating that the potential of their place of origin is close to the source anode potential and the other with higher energies originating around a potential hill in the source itself. Contributions of the two groups to the total current depend on source parameters and the cup bias; ion spectra from a cup at the anode potential are wider and have a more pronounced high energy group, while ions from a cup with a negatively biased or floating walls have a narrower spectrum close to the anode potential. Program BEAM can treat only a single Maxwellian ( $T_i$ ) ion energy distribution with or without a common shift toward higher energies ( $V_i$ ) in the direction parallel to the beam axis. This is necessarily an approximation, but for a cup with floating walls, it is satisfactory.

Of the two parameters ( $T_i, V_i$ ), the directed component represented by  $V_i$  was more critical, whilst runs made with different values of  $T_i$  (0.6 eV and 1 eV) gave very similar results. As described in Ref. 7, the Maxwellian ion temperature  $T_i$  enters into the calculation of the initial momenta of ions at the emitting surface. The effects of changing values of  $V_i$  cannot be separated from the influence of the other two parameters,  $T_e$  and  $m_\ell$ . As mentioned before, the drift velocity has been calculated in the program using the expression

$$v_D = \sqrt{\frac{2e}{m_i}} \left[ I(\eta_s) \exp(\eta_s) \sqrt{T_e} + \sqrt{V_i} \right] ,$$

where both  $T_e$  and  $V_i$  appear, expressed in volts. The plasma density required to deliver the assumed current density at  $r = 0$  is equal to

$$n_{eo} = \frac{j_+(\eta_s)_{r=0} \exp(\eta_s)}{e v_D} ,$$

while the Debye length  $\lambda_D$  is given by

$$\lambda_D = \frac{\sqrt{T_e}}{\sqrt{n_{eo}}} \cdot \frac{\sqrt{\epsilon_0}}{e} ,$$

where again  $T_e$  is expressed in volts. By substituting  $n_{eo}$  and  $v_D$ , one obtains

$$\lambda_D^2 \propto \frac{I(\eta_s) \exp(\eta_s) T_e^{3/2} + T_e \sqrt{V_i}}{\exp(\eta_s) j_+(\eta_s)_{r=0}} .$$

If for a certain geometry a good match has been found between the plasma and the outside electrostatic field (a proper value of the constant  $m_\ell$ ), then any change in  $T_e$ ,  $V_i$  or  $j_+(\eta_s)_{r=0}$  should be accompanied by a correction of the value of  $m_\ell$  as well. As a first approximation, one can assume that the position of the emitting surface does not move, therefore the value of  $m_\ell$  has to be inversely proportional to  $\lambda_D$ . However, any change in  $\lambda_D$  will be reflected in the axial mesh configuration as well; a smaller  $\lambda_D$  will result in a reduction of the step size in the vicinity of the plasma boundary (assuming that  $m_s$  remains constant). It is interesting to compare Figs. 5 and 6; the former shows the emittance vs. current for three values of  $V_i$  (10 V, 30 V, 50V) with a constant  $m_\ell$  equal to 50, while the latter shows the same relationship but with  $m_\ell$  corrected in such a way as to maintain the plasma boundary more or less at the same position. The difference between the curve for  $V_i = 50$  V and the other two curves for lower voltages on Fig. 5 is due mostly to the shift of the plasma boundary outwards when lowering  $V_i$ . This is also evident from Fig. 7, where  $m_\ell$  was used as parameter. On the other hand, there was very little difference between curves for  $V_i = 10$  V, 30 V or 50 V with  $m_\ell$  corrected as explained before (Fig. 6).

### 2.3.3 Ion Optical System Parameters

When analyzing the effects of plasma on beam characteristics, a certain geometry of the dc column has to be established a priori. The dc column is of the three-electrode, accel-decel type as schematically shown on Fig. 1. The potential difference and the distance between electrodes 1 and 2 have to be adjusted according to the desired beam intensity. As a first guess, the Child-Langmuir formula for the planar geometry can be used

$$d^2 = \frac{4}{9} \epsilon_0 \sqrt{\frac{2e}{m_i}} \frac{(U_2 - U_1)^{3/2}}{j} ,$$

where  $d$  is the distance between equipotentials  $U_1$  and  $U_2$  on the axis and  $j$  the required current density. Of course, the position of equipotentials on the axis is known only after running the program BEAM; therefore, the design of the preinjector is an iterative process. To obtain the desired beam intensity, a compromise must be found between the current density and the area of the plasma boundary exposed to the extraction field. The expression above gives an estimate for the distance between the equipotentials 0 and 90 kV on the axis of about 3 cm assuming a current density<sup>10</sup> of 0.16 A/cm<sup>2</sup>. Analyzing various geometries we have found that Pierce geometry is not applicable under our conditions because it holds for a well-defined emitter (not sheath) and a rectangular beam.

An initial set of studies done for different shapes of the first and second electrodes, as well as the experience of others, led to the selection of geometry, shown in Fig. 3, as the reference system for further shape optimization and plasma parameter study. The peculiar shape of the first electrode has been suggested by R. Keller, then at GSI, Darmstadt. It is this shape which brought substantial advantages in  $E(I)$ , as compared to the usual Pierce geometry. The "reference" shape has been obtained after an extensive computer optimization.

Effects of the initial angles of the first electrode have been compared for two values:  $59^\circ$  and  $42^\circ$  with respect to the horizontal axis (Fig. 8). A larger angle results in a slightly more intense beam but with a much higher emittance. In either case, the first electrode was extended with the same slope up to the end. Similarly, Fig. 9 shows again the effects of the initial slope, but with the slope being cut off at the same horizontal position as in the reference system. Angles with the horizontal axis were this time  $29^\circ$ ,  $42^\circ$ ,  $51^\circ$  and  $59^\circ$ . Results differed very little, with the exception of the largest angle, which gave a beam of poorest quality. Further, although not substantial, improvement was achieved with a shape approaching a smoother curve (also shown in Fig. 9), but it was considered doubtful that real benefits would justify such a complicated form of the electrode.

As mentioned before, the RFQ2 preinjector accelerates particles to an energy of 90 keV. This corresponds to the voltage difference of 90 kV between the first electrode and the ground electrode<sup>3</sup> of the dc column. The middle electrode (focus electrode) is usually put on a slightly negative potential,  $-V_f$ , (with respect to ground) in order to give a focusing effect to the beam. Several values of  $V_f$  have been tried out in the range of 0 to -10 kV. Best results were obtained for  $V_f$  between -5 and -7.5 kV. The graphs presented in various figures of this report refer to  $V_f = -5$  kV.

In Figs. 10 and 11 are represented some of the outputs of the program BEAM. The emittances in Fig. 11 are computed from the rms values of particle positions and angles:

$$E_x = E_y = 4E_{rms} \quad ,$$

where  $E_{rms}(x,x')$  (or  $E_{rms}(y,y')$ ) is the rms emittance

$$E_{rms}^2 = \overline{x^2} \overline{x'^2} - (\overline{xx'})^2 \quad .$$

Note that BEAM works with  $r$  and  $r'$  and relations hold:

$$\overline{x^2} = \frac{\overline{r^2}}{2} ,$$

$$\overline{x'^2} = \frac{\overline{r'^2}}{2} ,$$

$$\overline{xx'} = \frac{\overline{rr'}}{2} ,$$

because there are no azimuthal velocity components in the beam.

### 3. Determination of the preinjector and conclusion

The preinjector of the RFQ2 has been extensively studied according to procedures outlined in the previous chapter. A variety of electrode shapes has been analyzed and for each of them one tried to position correctly the plasma emitting surface. The ion current density distribution on the emitting surface corresponded to measurements on the CERN DP ion source.<sup>10</sup> After many trials one ended up with an optimized geometry, which was called the "reference" geometry. This geometry was then, in turn, further analyzed with respect to changes of the potential of the focus electrode and of the ion density distribution on the emitter surface. Satisfactory results were found concerning the size and form of the beam emittance at the end of the preinjector. The beam was suited to be transported further through appropriately placed focusing elements and injected into the RFQ.

Following the "reference" geometry, the preinjector for the RFQ2 has been constructed and put on the test stand in the autumn of 1987. A good agreement between computations and beam measurements was found, but this does not enter into the subject of this report.

### 4. Acknowledgment

C. Biscari, now at Laboratori Nazionali di Frascati, Italy, and A. Lombardi put the program BEAM into operation at CERN and introduced the required modifications. Various problems were discussed with B. Hamm, K. Crandall, and R. Keller. We thank them all.

References

1. J.S. Hornsby, A Computer Programme for the Solution of Elliptic Partial Differential Equations, CERN 63-7.
2. J.E. Boers, SNOW - A Digital Computer Program for the Simulation of Ion Beam Devices, Sandia National Laboratories SAND-1029 (August 1980).
3. M.B. Shubaly, R.A. Judd, and R.W. Hamm, BEAM, An Improved Beam Extraction and Acceleration Modeling Code, IEEE Trans. on Nuclear Science, Vol. NS-28, No.9, June 1981.
4. R. Hamm, R. Judd, and M. Shubaly, BEAM - Version 1.0 (draft), Appl. Math. Branch, Chalk River Nuclear Laboratories, Ontario, Canada (October 1981).
5. R.W. Hamm, BEAM Input Description, AT-1-81-123, LANL, Los Alamos, USA (April 1981).
6. T. Bulirsch and J. Stoer, Numerische Mathematik 8, 1 (1968).
7. E.F. Jaeger and J.C. Whitson, Numerical Simulation for Axially Symmetric Beamlets in the Duopigatron Ion Source, ORNL - TM-4990, Oak Ridge National Laboratory, USA (August 1975).
8. S.A. Self, Exact Solution of the Collisionless Plasma-Sheath Equation, Phys. Fluids, 6, 1762 (1963).
9. D. Bohm, A. Guthrie, and R.K. Wakerling, The Characteristics of Electrical Discharges in Magnetic Fields, eds.; McGraw-Hill, New York (1949)



10. J. Grando, Caracteristiques du Plasma Emissif de la Source Duoplasmatron, CERN/PS/LR 79-21 (June 1979).
11. C. Gautherin, C. Lejeune, F. Prangere and A. Septier, Etude des Spectres d'Energie des Particules Chargées Emises par une Décharge du Type Duoplasmatron, Plasma Physics 11, 397 (1969).
12. F.M. Bacon, Gas Discharge Ion Source. 1. Duoplasmatron, Rev. Sci. Instr. 49 (4), (April 1948).

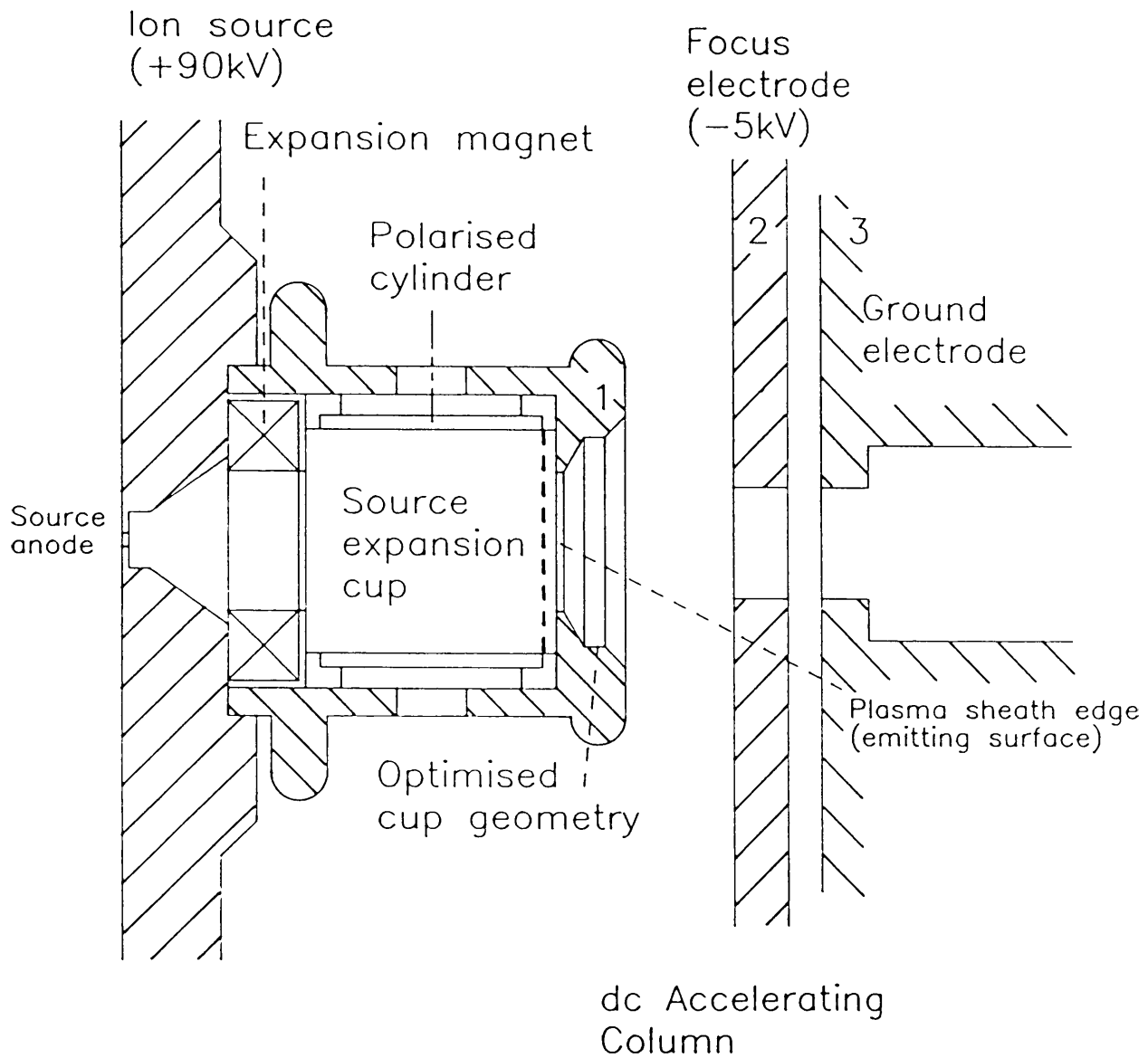


Fig. 1 Sketch of the duoplasmatron extraction geometry and acceleration electrodes.

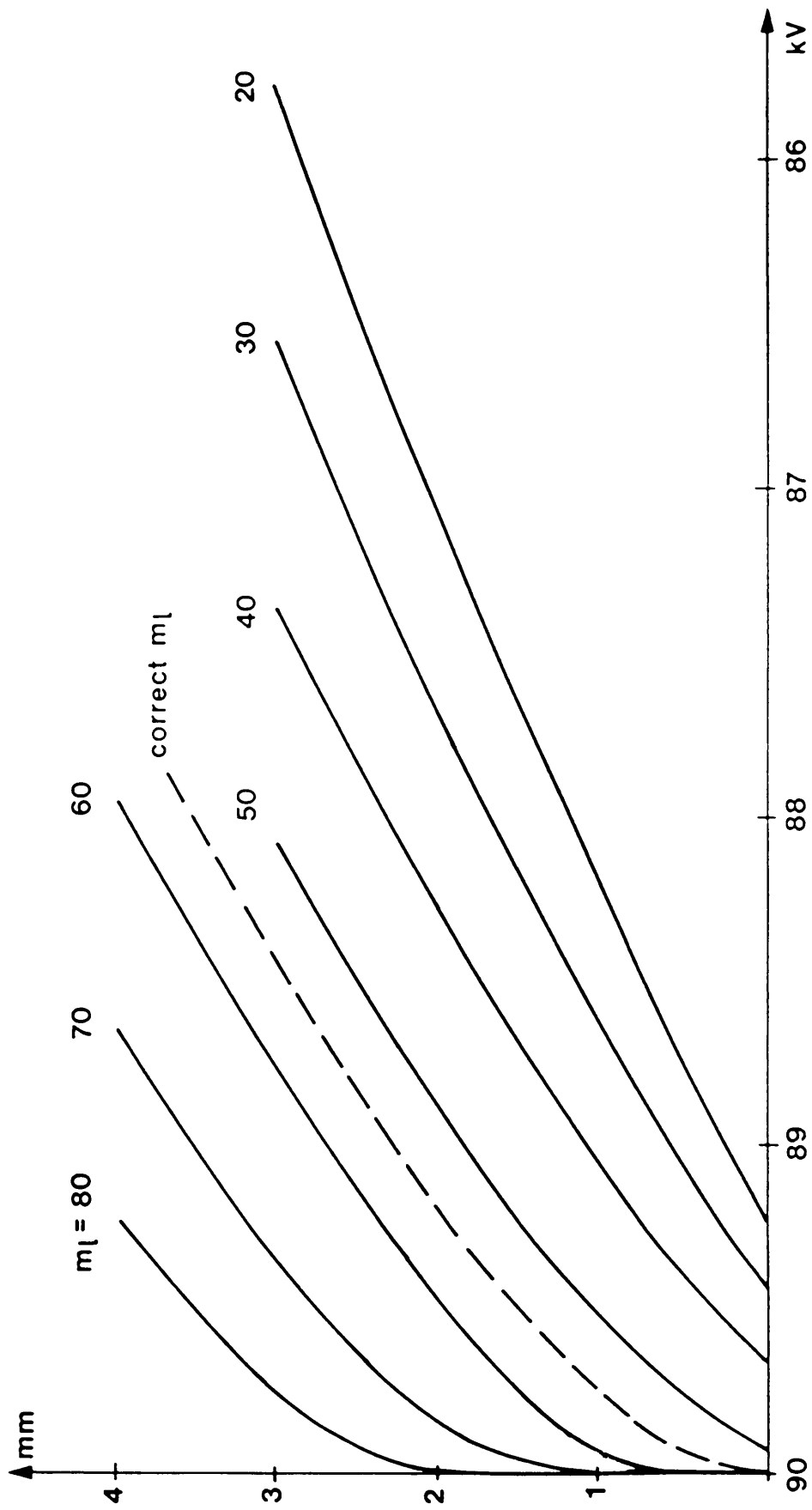


Fig. 2 Computed equipotentials in the neighborhood of the plasma boundary with  $m_l$  as parameter.

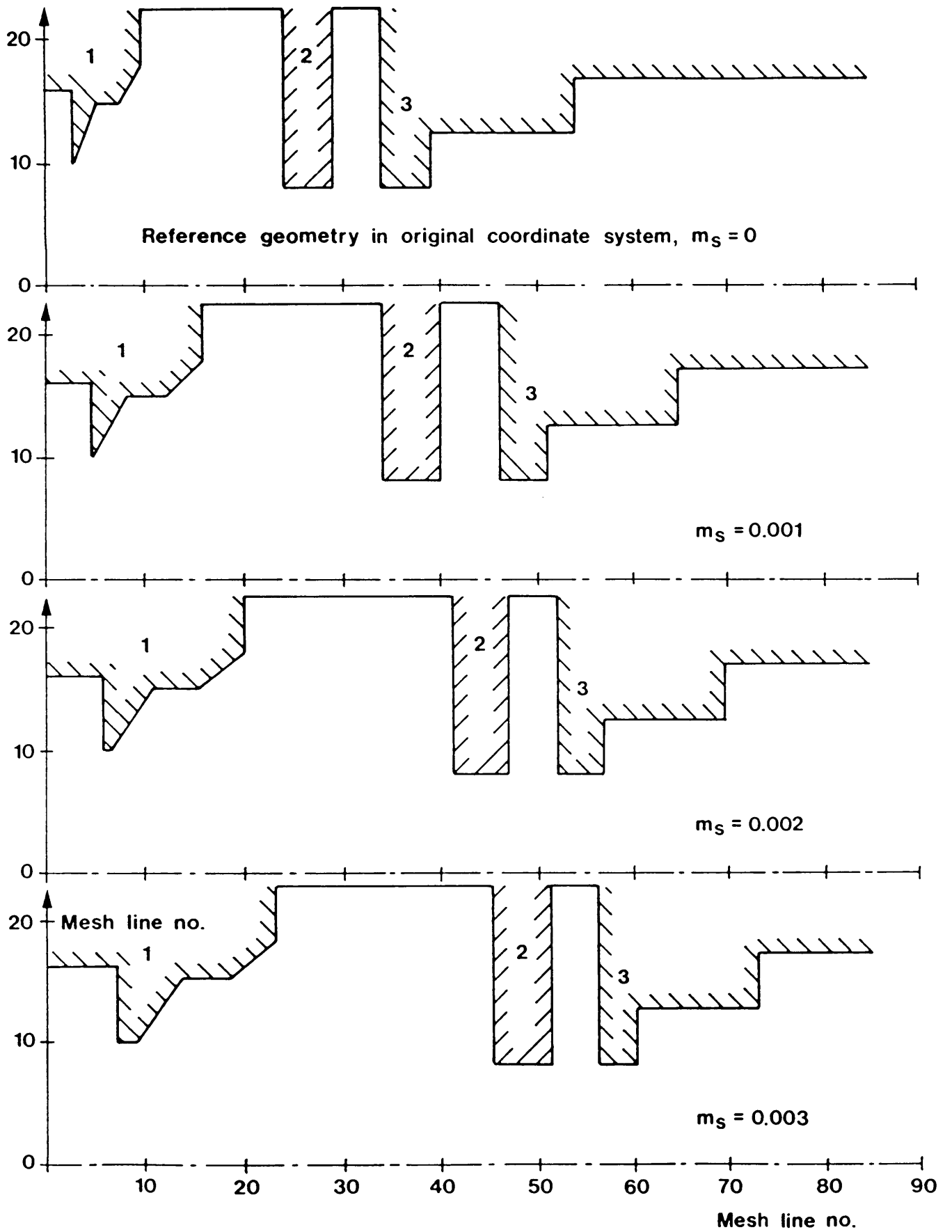


Fig. 3 RFQ2 preinjector presented in various coordinate systems specified by  $m_s$ .

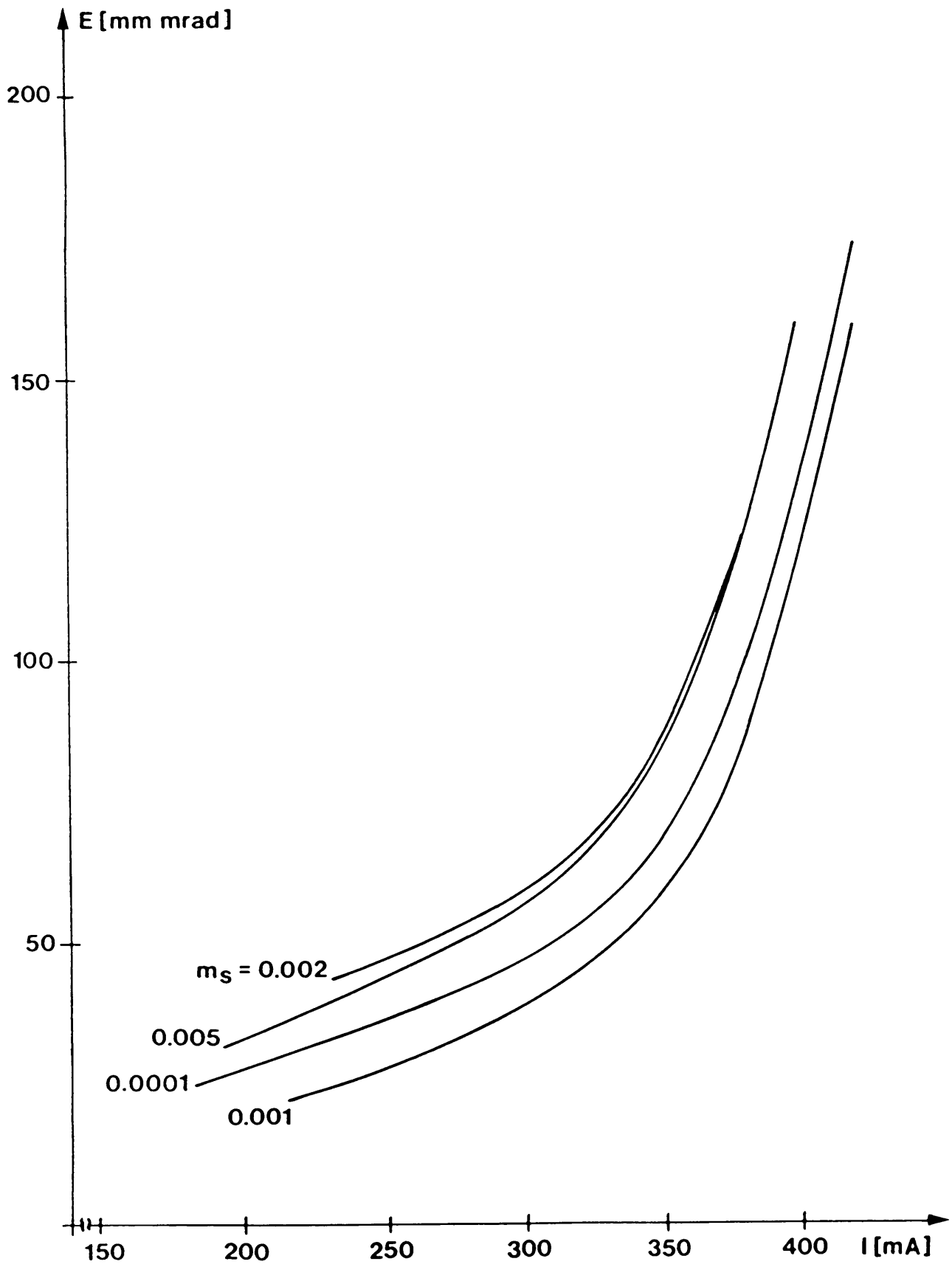


Fig. 4 Beam emittances  $E(I)$  with  $m_s$  as parameter.

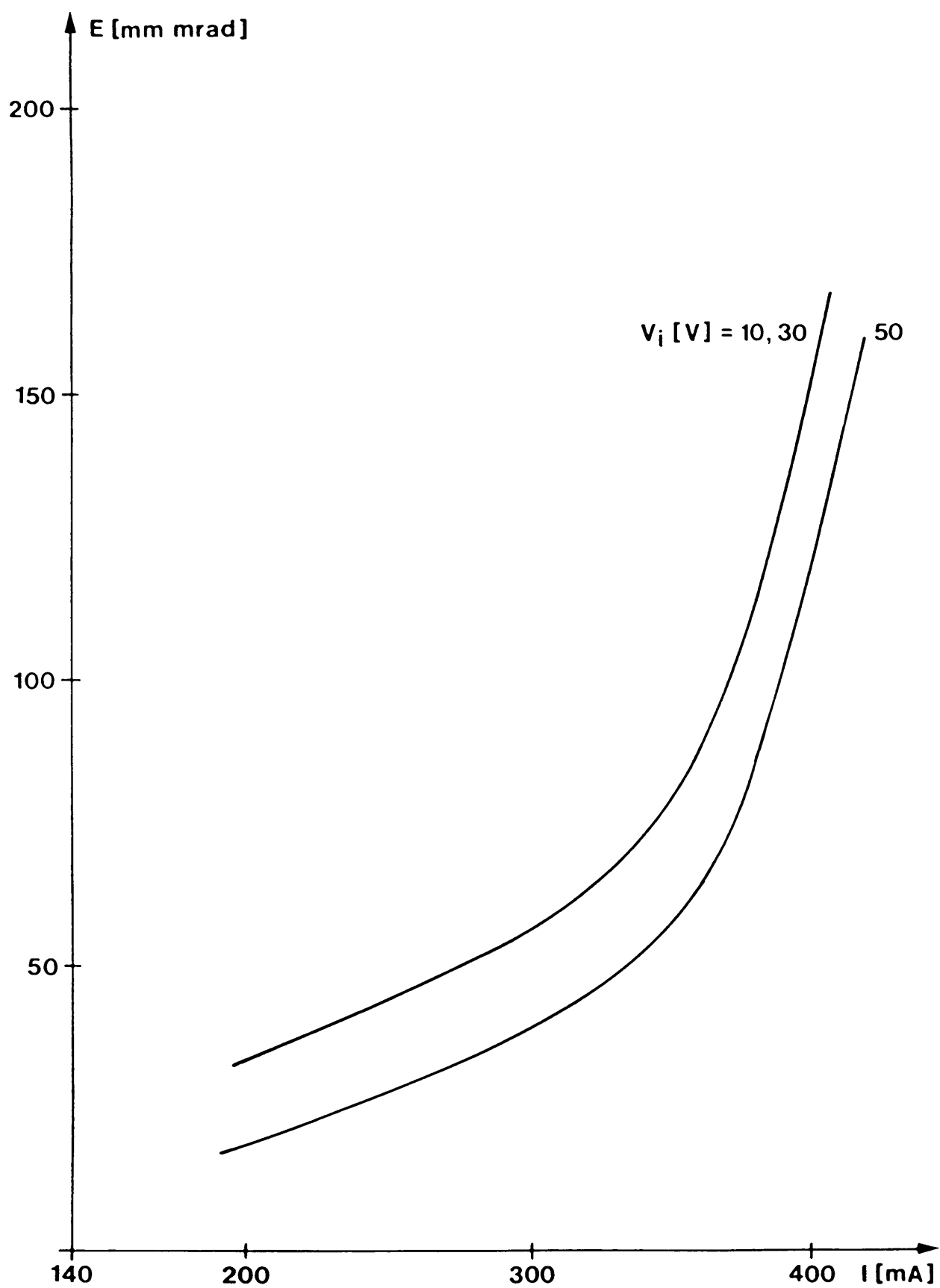


Fig. 5 Beam emittances,  $E(I)$ , with  $V_i$  as parameter;  $m_\ell = \text{const.} = 50$ .

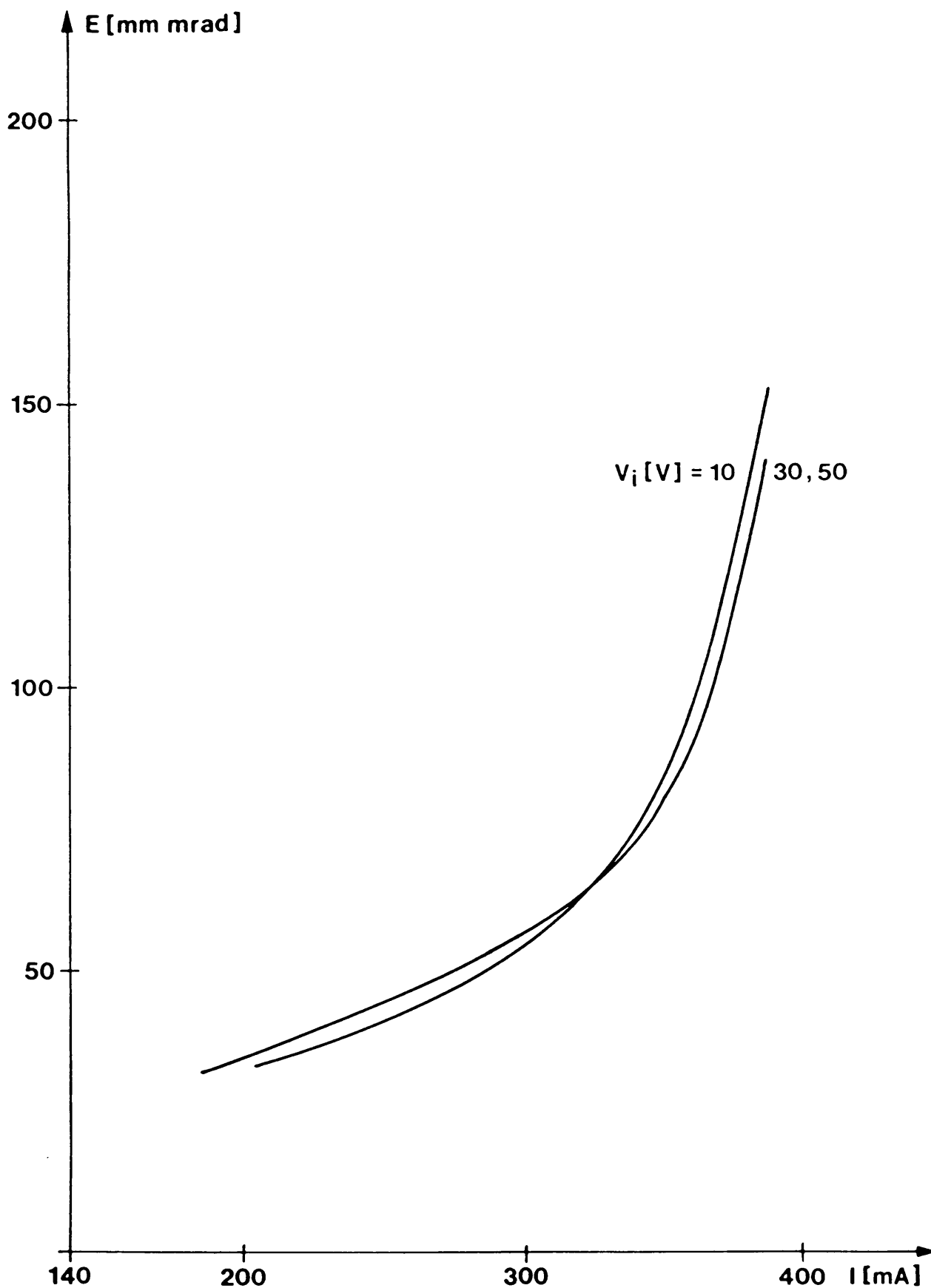


Fig. 6 Beam emittances,  $E(I)$ , with  $V_i$  as parameter;  $m_\ell$  varied to keep the product  $m_\ell \lambda_D = \text{const.}$

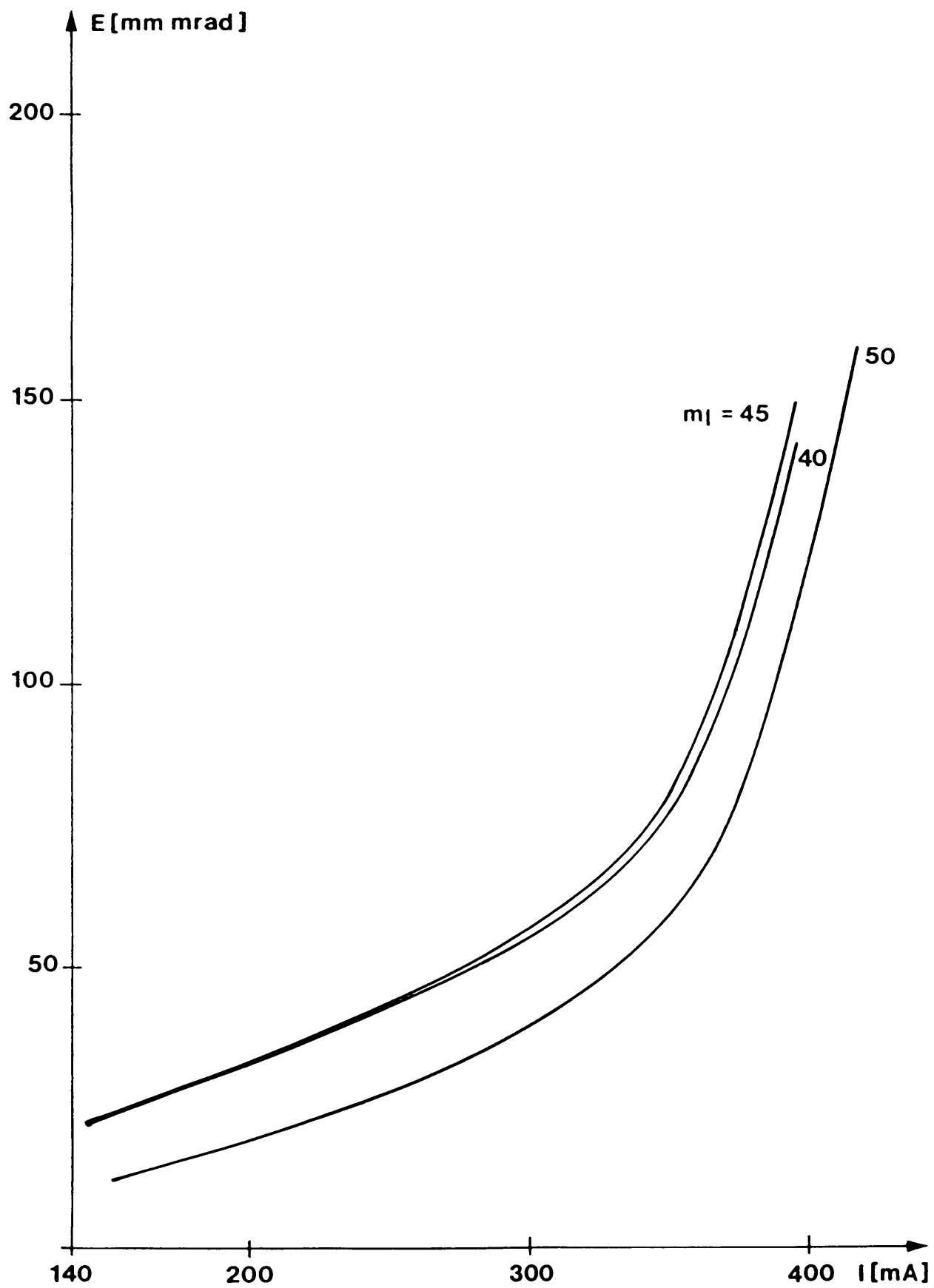


Fig. 7 Beam emittances,  $E(I)$ , with  $m_l$  as parameter;  $V_i = \text{const.} = 50 \text{ V.}$



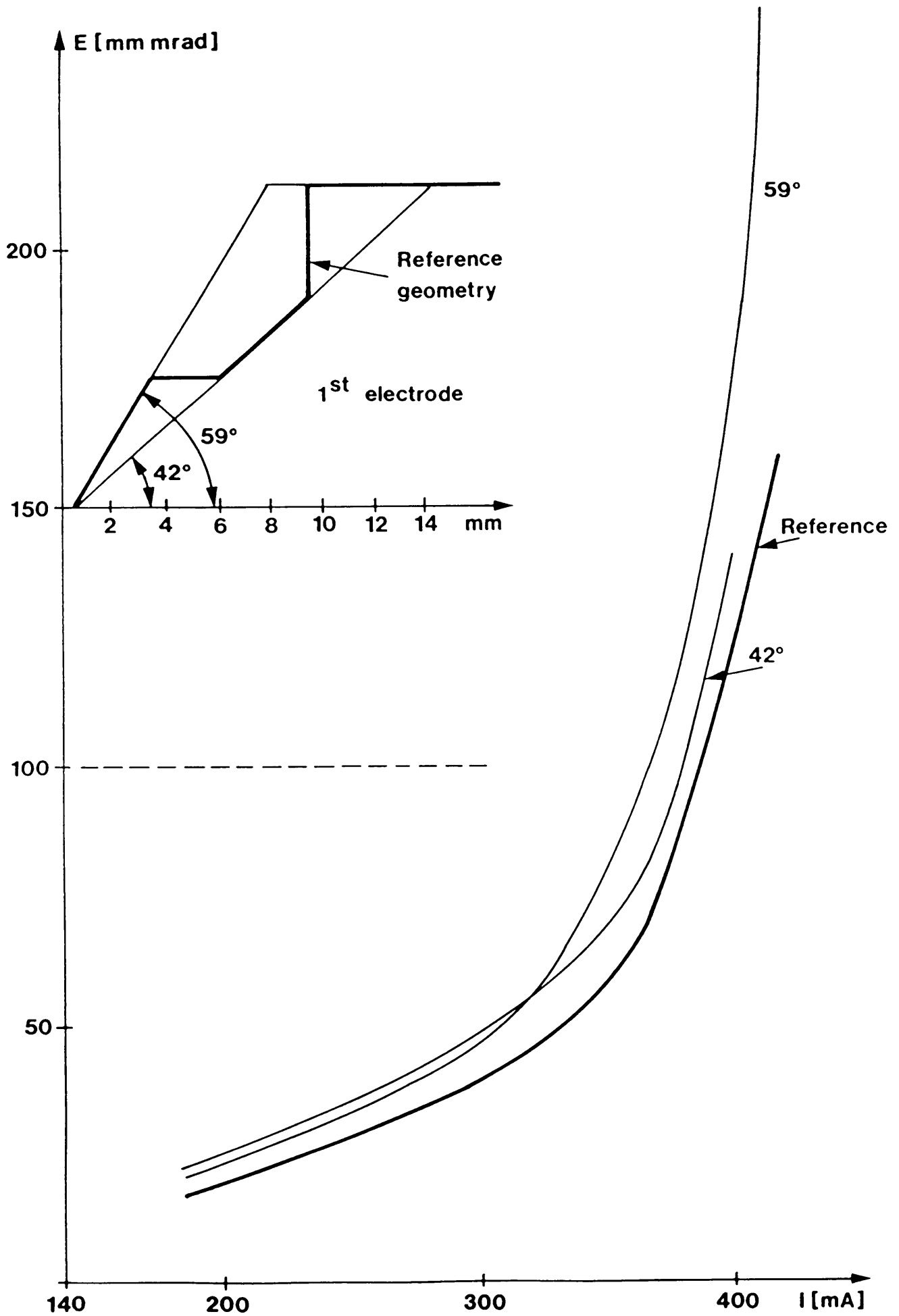


Fig. 8 Beam emittances,  $E(I)$ , with the angle of first electrode as parameter.

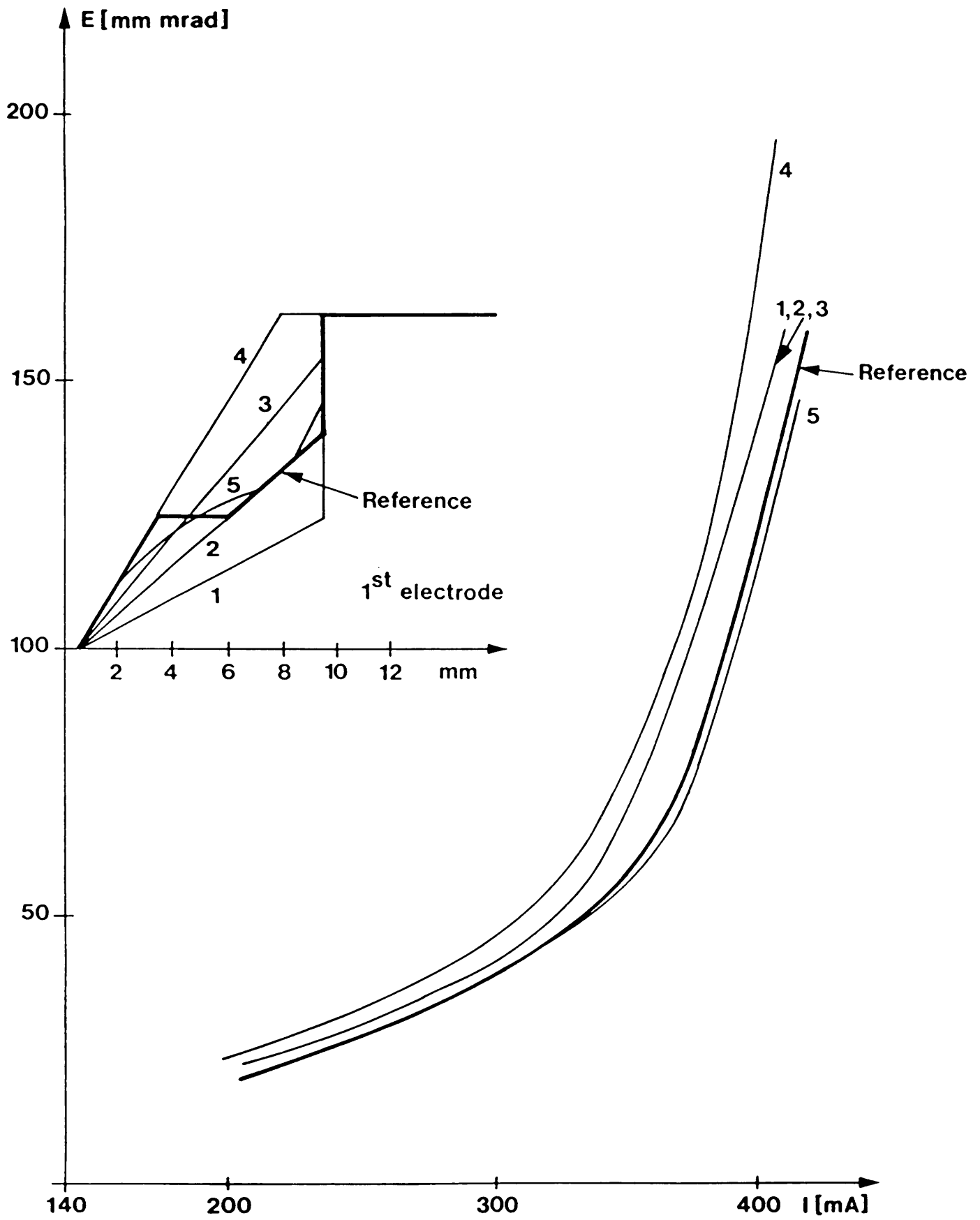


Fig. 9 Beam emittances  $E(I)$ , with the shape of first electrode as parameter.

RFQ2 - ANALYSIS OF PREINJECTION

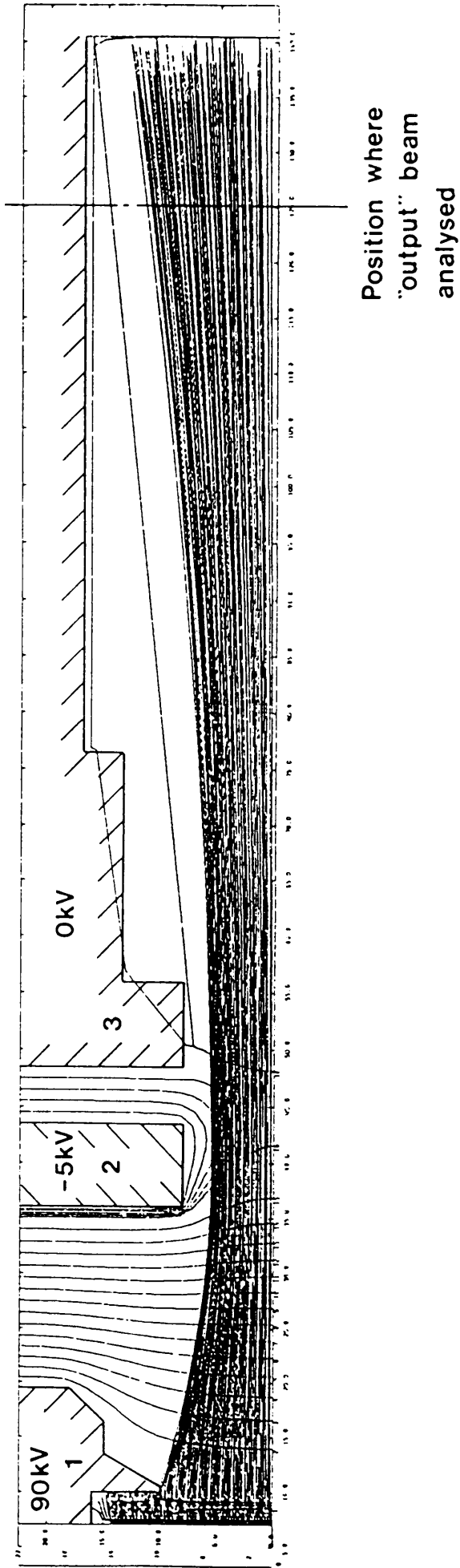
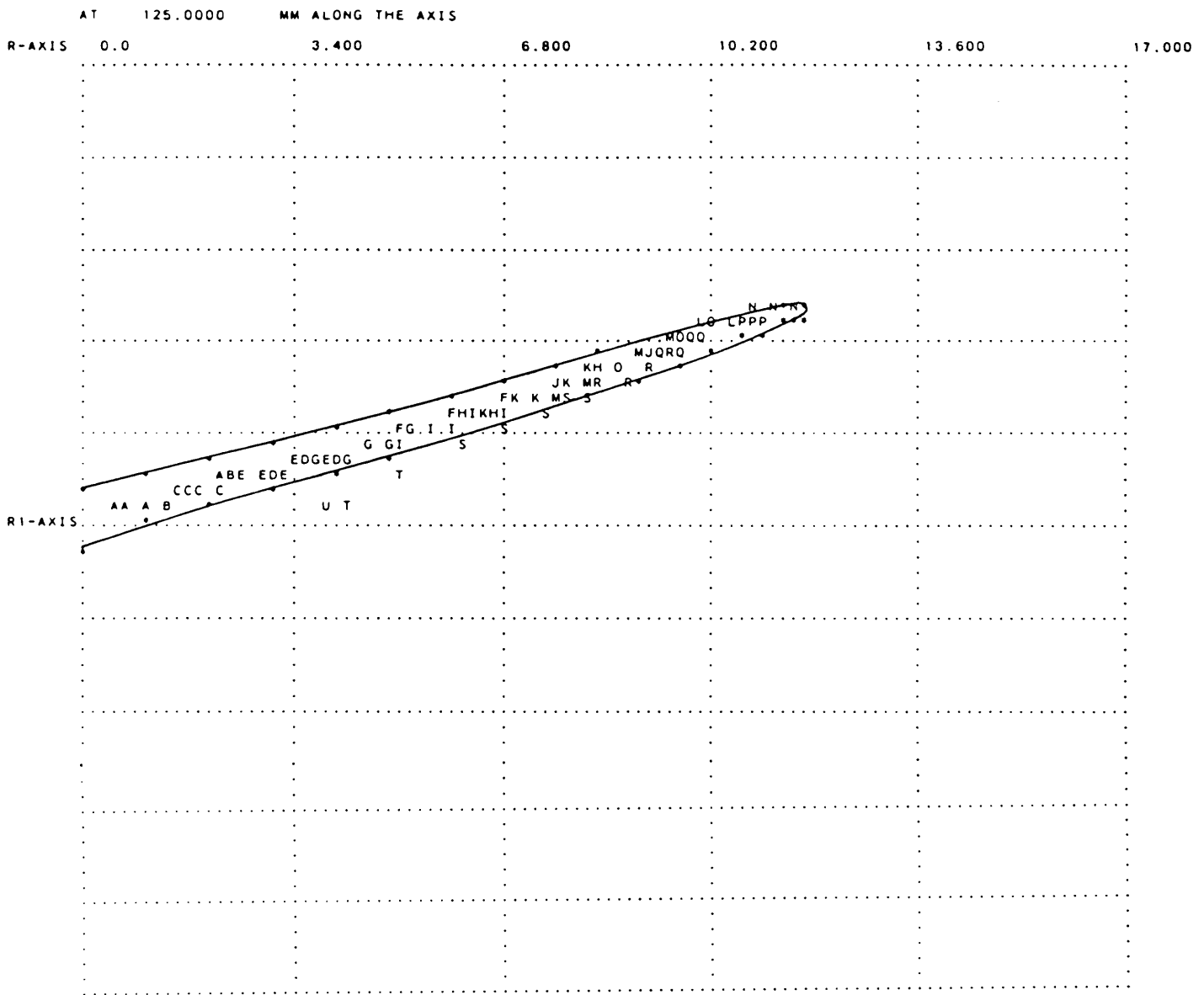


Fig. 10 Particle trajectories and equipotentials as computed by program BEAM.



EQUIVALENT BEAM PARAMETERS

FOR 98 PARTICLES - CURRENT = 0.3983529 AMP  
 RADIUS (2\*RMS) = 10.21977 MM , DIVERGENCE (2\*RMS) = 99.20918 MRAD  
 EMITTANCE (4\*RMS) = 148.0346 PI-MM-MRAD  
 ALPHA = -9.077138 , BETA = 0.9407149 , GAMMA = 88.65007

RELATION BETWEEN CURRENT AND EQUIVALENT EMITTANCE

RAY	ND	ALPHA	BETA	EMITTANCE	FRAC	CURRENT	FRAC	BRIGHTNESS
98	97	-9.08	0.941	148.021	1.000	0.398353	1.000	0.456E-04
93	90	-14.32	1.463	99.301	0.671	0.370077	0.929	0.942E-04
88	88	-19.25	1.942	75.832	0.512	0.339018	0.851	0.148E-03
83	65	-21.53	2.183	65.204	0.441	0.311974	0.783	0.184E-03
78	56	-22.68	2.323	56.956	0.385	0.282984	0.710	0.219E-03
73	64	-23.63	2.443	50.722	0.343	0.254965	0.640	0.249E-03
68	60	-24.72	2.579	45.028	0.304	0.228321	0.573	0.283E-03
63	55	-25.90	2.734	37.835	0.256	0.199433	0.501	0.350E-03
58	40	-26.30	2.813	31.725	0.214	0.169987	0.427	0.424E-03
53	51	-28.19	3.035	27.848	0.188	0.147573	0.370	0.478E-03
48	47	-30.85	3.369	21.552	0.146	0.123081	0.309	0.665E-03
43	29	-34.73	3.831	16.815	0.114	0.103253	0.259	0.917E-03
38	22	-42.50	4.657	14.431	0.097	0.086636	0.217	0.104E-02
33	1	-60.20	6.556	10.886	0.074	0.071687	0.180	0.152E-02
28	12	-78.79	8.564	8.902	0.060	0.063650	0.160	0.202E-02

Fig. 11 Characteristics of output beam with half-emittance plot (4 •  $E_{rms}$ ) as computed by program BEAM.